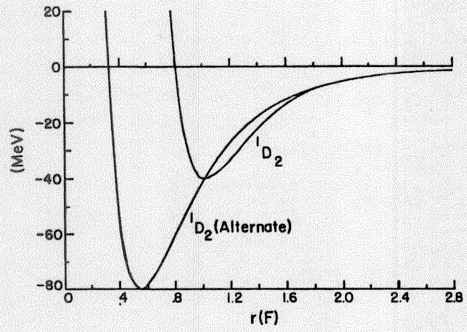

FIG. 5. The soft core and alternate soft core $^1D_2$ potentials.

would be much too attractive: we have the same phenomenon as in the $^1D_2$ state. It is evident that our procedure, of choosing directly the effective potential for the $^3D_2$, is no different from that of Yale and HJ. A difference would occur if we went on to the $^3G_4$ because for this state we would again determine a new effective potential: but here, as for many states of high L and J, the experimental information is meager.

The only remaining state is the $^3P_0$. The Yale or HJ form predicts the effective potential here from the V_C, V_T and V_{LS} determined in the $^3P_2 - {}^3F_2$ state while our $^3P_0$ is independent. Figs. 3 and 4 and Table XII show that our $^3P_0$ potential is actually in qualitative agreement with the behavior expected from the potential components of the triplet $J = 2$ state. This agreement could be improved, but our over-all fit would suffer. We therefore kept the $^3P_0$ potential independent.

Apart from this state the choice of different potentials for each TSJ does not differ essentially from the procedure of Yale and HJ provided we ignore all states of $J \geqslant 3$. In fact, potentials of the HJ and Yale form are assumed to be the OPEP alone for $L > 5$ and even for $L \leqslant 5$ the Yale potential uses (3) for triplet-odd states with $J \leqslant 2$ but puts $V_{LS} = 0$ for $J > 2$. This sudden change will be explained in Section IV where we further discuss requirements made on the functional form of the potential by the data.

Since the longest range part of the NN interaction is known to be the OPEP (see Eq. 6) our potentials have it for their tail. In the OPEP g^2 was taken to be 14 and a short range interaction was subtracted from its tensor part to remove the x^{-2} and x^{-3} behavior at small x. At intermediate distances the potential was represented by sums of convenient Yukawas of the form $\exp(-nx)/x$ where n is an integer. No attempt was made to make nm_π correspond to the mass of a known particle. We expressed the short range repulsion by means of both hard (infinitely hard) and soft (Yukawa) cores. Our Yukawa cores are soft in the sense that wave functions do not vanish inside them at nonzero radii. They are too strong to be treated as a perturbation; the Born approximation, for example, generally fails. Two-nucleon data do not distinguish between hard and soft cores.[4] It is to be hoped that properties of large nuclei and nuclear matter will shed light on the short range behavior.

In the Schrödinger equation we use

$$\hbar^2/M = 41.47 \text{ MeV–F}^2$$

and

$$Me^2/(\mu^2\hbar^2 r) = .049602/x$$

where

$$x = \mu r$$

with

$$\mu = .7F^{-1}$$

If $\mu = mc/\hbar$ then the pion mass, m, is about 138.13 MeV. The nucleon mass, M, is about 938.903 MeV which is close to twice the reduced np mass.

For an uncoupled state with potential $V(x)$ and orbital momentum L the Schrödinger equation is

$$[d^2/dx^2 + K^2 - L(L+1)/x^2 - \epsilon/x - U(x)]\, u(x) = 0 \tag{8}$$

where

$$K^2 = ME/(\mu^2\hbar^2)$$

$$\epsilon = \begin{cases} .049602 & \text{if the Coulomb potential is present} \\ 0 & \text{otherwise} \end{cases}$$

and

$$U(x) = MV(x)/(\mu^2\hbar^2).$$

For a coupled state with total angular momentum J and potential

$$V = V_C(x) + V_T(x)\, S_{12} + V_{LS}(x)\, \mathbf{L}\cdot\mathbf{S}$$

[4] Bressel, Kerman, and Lomon (*25*) demonstrated this by fitting pp data with the HJ potential whose hard core was replaced by larger-radius, finite, flat-topped cores. Bressel, Kerman and Rouben (*26*) have improved the model and extended it to include the np case.

the Schrödinger equation is

$$\begin{aligned}
&[d^2/dx^2 + K^2 - J(J-1)/x^2 - \epsilon/x - U_C(x) + 2(J-1)\,U_T(x)/(2J+1) \\
&\qquad - (J-1)\,U_{LS}(x)]\,u(x) \\
&\quad = \{6[J(J+1)]^{1/2}/(2J+1)\}\,U_T(x)\,w(x) \\
&[d^2/dx^2 + K^2 - (J+1)(J+2)/x^2 - \epsilon/x - U_C(x) + 2(J+2)\,U_T(x)/(2J+1) \\
&\qquad + (J+2)\,U_{LS}(x)]\,w(x) \\
&\quad = \{6[J(J+1)]^{1/2}/(2J+1)\}\,U_T(x)\,u(x)
\end{aligned} \tag{9}$$

where $U_C(x) = MV_C(x)/(\mu^2\hbar^2)$ and likewise for U_T and U_{LS} and $u(w)$ is the wave function for the $L = J-1$ ($L = J+1$) channel.

III. RESULTS. THE POTENTIALS AND THEIR PROPERTIES

For historical reasons the hard and soft core potentials were fit to different sets of phases. We simply used the best available at the time the work was done. For the hard core model we used YRB1(K_0) (*27*) for isotopic spin (T) one states and YLAN4MP (*27*) for $T = 0$. These are late 1964 Yale phases. The $T = 1$ soft core potentials were fit to the results of a 58 parameter energy-dependent analysis of Arndt and MacGregor (*24*) and the $T = 0$ to results of a similar analysis done in late 1966 (*28*).

When one fits phase parameters rather than the scattering data itself there is always the danger the correlated errors will destroy the fit of the potential to the data. Yoder and Signell (*29*) compared our hard core, but not our soft core $T = 1$ potential to *pp* scattering data in the range 10 to 330 MeV. They used our model where we specify it and at our suggestion, the OPEC alone in all other states (those with $J > 2$). They found that this procedure gave a χ^2 of 2.9 times the number of data (652) whereas a later, improved version of the phases to which we fit (YRB1) gave 2.1. Even though the figure 2.9 depends strongly on the particular collection of data used it implies a reasonable prediction of scattering behavior. Moreover, deviations from the OPEC[5] in some higher angular momentum states, where we give no potentials, make a considerable difference in *NN* scattering. Use of the OPEC alone in these states represents a handicap which is, of course, reflected in the fit to the data by our potential. We believe that it could be greatly improved by a few refinements but that properties of nuclei would be insensitive to these adjustments in the potential. Finally we note that of all potentials examined in Reference (*29*) ours gave the best fit to the data.

[5] The previously mentioned $^3F_4$ phase is a striking example.

A. Isotopic Spin One

$T = 1$ phase shifts can be extracted from *pp* scattering data alone. This is useful because there is not enough accurate *np* data by themselves to determine both $T = 1$ and $T = 0$ phases simultaneously and there is very little quantitative information regarding the *nn* interaction. However, phases obtained using *pp* scattering are complicated by the fact that they are shifts in the phases of Coulomb wave functions caused by the combined effect of Coulomb and nuclear forces.[6] Thus we are forced to calculate $T = 1$ phase shifts by integrating a Schrödinger equation whose potential is the sum of the Coulomb and *NN* potential. At a radius large enough for the *NN* potential to be negligible we fit the solution to Coulomb wave functions to get the phase.

Hard core $T = 1$ potentials are given in Eqs. (10) through (14) where $h = 10.463$ MeV, from the OPEP. The hard core radius, x_c, is .29614 in the ^1S state and .3 in the others.

$$V(^1S) = -h(e^{-x} + 39.633e^{-3x})/x \tag{10}$$

$$V(^1D) = -h(e^{-x} + 4.939e^{-2x} + 154.7e^{-6x})/x \tag{11}$$

$$V(^3P_0) = -h(G_1 + 16.2e^{-2x} - 55.6e^{-3x} - 545e^{-6x})/x \tag{12}$$

where

$$G_1 = (1 + 4/x + 4/x^2)\,e^{-x} - (24/x + 4/x^2)\,e^{-6x}$$

$$V(^3P_1) = h(G_2 - 1.1553\,e^{-2x} - 8.722\,e^{-3x} + 175.1\,e^{-6x})/x \tag{13}$$

where

$$G_2 = (1 + 2/x + 2/x^2)\,e^{-x} - (12/x + 2/x^2)\,e^{-6x}$$

$$V(^3P_2 - {}^3F_2) = V_C + V_T S_{12} + V_{LS}\mathbf{L}\cdot\mathbf{S} \tag{14}$$

where

$$V_C = h(e^{-x}/3 - 13.8e^{-3x} + 138e^{-6x})/x$$

$$V_T = h[(1/3 + 1/x + 1/x^2)\,e^{-x} - (6/x + 1/x^2)\,e^{-6x} - 5.688e^{-3x}]/x$$

$$V_{LS} = -250.9he^{-6x}/x$$

Recall that $x = \mu r$ with $\mu = .7F^{-1}$. The hard core radius was allowed to vary only in the ^1S state. Due to the angular momentum barrier, in other states x_c can float around wildly. The choice $x_c = .3$ was arbitrary. An alternate ^1D potential with the ^1S core, $x_c = .29614$ is

$$V(^1D_2, \text{alternate}) = -h(e^{-x} + 25.86e^{-3x})/x \tag{15}$$

[6] There are other, less important electromagnetic and relativistic effects. See Breit (*20*) and Heller (*30*).

TABLE I

$T = 1$ HARD CORE PHASE PARAMETERS

E	$\delta(^1S_0$, radians)		$\delta(^1D_2$, radians)		
Lab, MeV	Potential	YRB1 (27)	Potential	YRB1	Alternate Potential
19.8	.882	.868	.009	.012	.008
50	.671	.670	.031	.033	.028
107	.403	.416	.068	.068	.066
170	.196	.198	.104	.102	.105
240	.018	.011	.140	.141	.142
310	−.128	−.132	.171	.175	.171
345	−.193	−.194	.186	.187	.182

E	$\delta(^3P_0$, radians)		$\delta(^3P_1$, radians)	
Lab, MeV	Pot.	YRB1	Pot.	YRB1
19.8	.151	.178	−.071	−.082
50	.233	.226	−.149	−.147
107	.174	.161	−.247	−.244
170	.057	.063	−.331	−.334
240	−.070	−.055	−.410	−.412
310	−.185	−.188	−.481	−.469
345	−.238	−.258	−.513	−.493

	$\delta(^3P_2$, radians)		$\rho_2 = \sin(2\epsilon_2)$		$\delta(^3F_2$, radians)	
Lab, MeV	Pot.	YRB1	Pot.	YRB1	Pot.	YRB1
19.8	.028	.029	−.020	−.028	.001	.001
50	.094	.099	−.056	−.071	.006	.006
107	.198	.205	−.089	−.093	.013	.011
170	.261	.260	−.095	−.095	.017	.009
240	.285	.276	−.089	−.093	.015	.005
310	.281	.275	−.080	−.085	.005	.001
345	.272	.273	−.075	−.080	−.002	−.002

Phase parameters ealculated from these potentials are given in Table I. We use only the nuclear bar (5) parameterization.

Soft core $T = 1$ potentials in MeV are given in Eqs. (16) through (20). Again $h = 10.463$ MeV and $x = \mu r$ with $\mu = .7\ F^{-1}$.

$$V(^1S) = -he^{-x}/x - 1650.6e^{-4x}/x + 6484.2e^{-7x}/x \tag{16}$$

$$V(^1D) = -he^{-x}/x - 12.322e^{-2x}/x - 1112.6e^{-4x}/x + 6484.2e^{-7x}/x \tag{17}$$

$$V(^3P_0) = -h[(1 + 4/x + 4/x^2)\, e^{-x} - (16/x + 4/x^2)\, e^{-4x}]/x + 27.133e^{-2x}/x - 790.74e^{-4x}/x + 20662e^{-7x}/x \tag{18}$$

$$V(^3P_1) = h[(1 + 2/x + 2/x^2)\, e^{-x} - (8/x + 2/x^2)\, e^{-4x}]/x - 135.25e^{-2x}/x + 472.81e^{-3x}/x \tag{19}$$

$$V(^3P_2 - {}^3F_2) = V_C + V_T S_{12} + V_{LS}\mathbf{L}\cdot\mathbf{S} \tag{20}$$

where

$$V_C = \frac{h}{3} e^{-x}/x - 933.48\, e^{-4x}/x + 4152.1\, e^{-6x}/x$$

$$V_T = h[(1/3 + 1/x + 1/x^2)\, e^{-x} - (4/x + 1/x^2)\, e^{-4x}]/x - 34.925\, e^{-3x}/x$$

$$V_{LS} = -2074.1\, e^{-6x}/x.$$

Two alternate potentials are

$$V(^1S, \text{Alternate}) = -he^{-x}/x + 105.32e^{-3x}/x - 2401.9e^{-4x}/x + 5598.2e^{-6x}/x \tag{21}$$

$$V(^1D, \text{Alternate}) = -he^{-x}/x - 318.64e^{-3x}/x + 526.27e^{-5x}/x \tag{22}$$

Phase parameters calculated from these potentials are given in Table II. The energies used in Table II are different from those of Table I because the YRB1 and AM parameters are tabulated by their authors at different energies. See Fig. 6–8 for comparisons of the phases. Our parameters were obtained by inserting a small fictitious hard core and integrating outwards. Any hard core radius $x_c \leqslant .01$ can be used.

The effective range expansion for an S-wave phase shift is (31)

$$k \cot \delta = -1/a + \tfrac{1}{2} r_e k^2 - P r_e^3 k^4 \tag{23}$$

where $k = (ME/2\hbar^2)^{1/2}$, E is the lab energy and it has been assumed that the Coulomb potential is absent.

TABLE II

$T = 1$ SOFT CORE PHASE PARAMETERS

E	δ (^1S, radians)			δ (^1D, radians)		
Lab, MeV	Potential	A–M (*24*)	Alternate Potential	Potential	A–M	Alternate Potential
24	.862	.868	.861	.011	.012	.011
48	.696	.686	.694	.027	.029	.027
96	.454	.445	.451	.059	.061	.059
144	.277	.278	.274	.089	.088	.089
208	.093	.101	.092	.123	.120	.121
304	−.118	−.115	−.115	.156	.159	.158
352	−.205	−.206	−.200	.164	.176	.171

E	δ ($^3P_0$, radians)	
Lab, MeV	Pot.	A–M
24	.141	.122
48	.198	.213
96	.179	.186
144	.105	.099
208	−.012	−.009
304	−.184	−.173
352	−.264	−.273

E	δ ($^3P_1$, radians)	
Lab, MeV	Pot.	A–M
24	−.074	−.074
48	−.133	−.132
96	−.228	−.228
144	−.304	−.306
208	−.386	−.387
304	−.479	−.477
352	−.518	−.514

E	δ ($^3P_2$, radians)		$\rho_2 = \sin(2\epsilon_2)$		δ ($^3F_2$, radians)	
Lab, MeV	Pot.	A–M	Pot.	A–M	Pot.	A–M
24	.038	.039	−.026	−.029	.002	.002
48	.093	.095	−.057	−.061	.005	.006
96	.186	.186	−.091	−.094	.013	.015
144	.243	.241	−.103	−.103	.018	.020
208	.277	.277	−.104	−.102	.022	.022
304	.282	.285	−.092	−.098	.019	.017
352	.274	.278	−.085	−.099	.014	.014

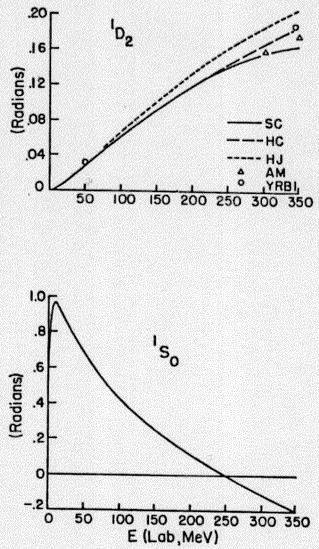

FIG. 6. $^1S_0$ and $^1D_2$ phase shifts. The soft core (SC) and hard core (HC) phases are from the corresponding potentials. The Hamada–Johnston (HJ) are taken from their paper (*11*). The Yale YRB1(K_0) (*27*) phases are plotted only when they differ significantly from those of the HC and the Arndt and MacGregor (AM) (*24*) when they differ from the SC. All the $^1S_0$ phases are in agreement to the accuracy of the plot.

TABLE III

^1S EFFECTIVE RANGE PARAMETERS FOR NO COULOMB POTENTIAL PRESENT

Potential	$a(F)$	$r_e(F)$	P
HC	−16.7	2.87	.018
SC	−17.1	2.80	.020
SCA	−17.1	2.80	.020

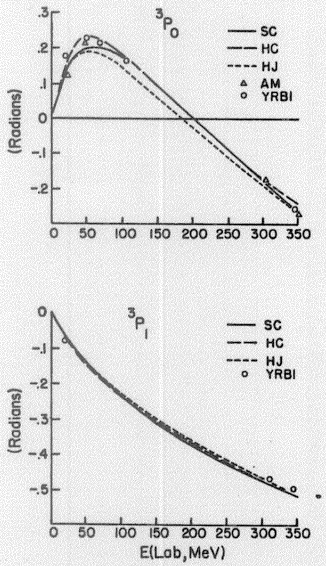

FIG. 7. $^3P_0$ and $^3P_1$ phase shifts. See caption to Figure 6.

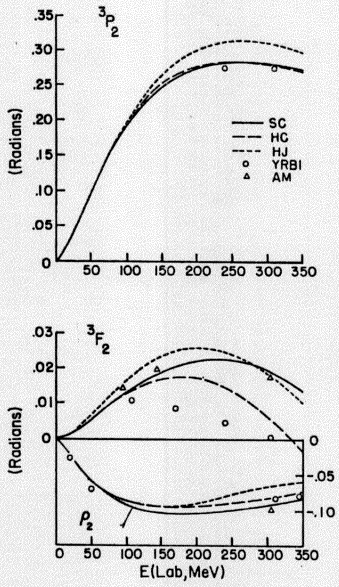

FIG. 8. $^3P_2$-$^3F_2$ phase parameters. See caption to Fig. 6.

Table III gives effective range parameters for the hard core (HC), soft core (SC) and alternate soft core (SCA) potentials calculated from (*23*) using three low energy phases.

Since charge independence claims that the nuclear *pp*, the *nn* and the spin singlet part of the *np* forces are all very nearly alike there are in principle, three experimental sources of data which with we can compare our parameters. Unfortunately, experimental *pp* phases are the result of the nuclear plus electromagnetic forces and it is very difficult to study the *nn* interaction (*32*). Using an approximate relation between the scattering length, a, with and without the Coulomb force, Heller, Signell and Yoder (*33*) find for the *pp* interaction, $a = -17F$. They also give $a = -16.8$ for the Yale potential and $-16.7F$ for the HJ. Haddock et al. (*34*) studied the reaction $\pi + d \to 2n + \gamma$ and obtained $a = -16.4 \pm 1.9F$ for the *nn* interaction. These values not only agree well with those from our potentials but also support the assumption of charge symmetry.

On the other hand, in an analysis of low energy *np* data Noyes (*35*) found that

for the spin zero part $a = -23.678 \pm .028F$ and $r_e = 2.51 \pm$ about $.15F$. Breit, Friedman and Seamon (*36*) looked carefully at the effects of possible systematic and other errors on the singlet *np* effective range, r_e, and concluded that a value larger than $2.70F$ was not at all excluded. Houk and Wilson (*37*) give $a = -23.714 \pm .013F$ and $r_e = 2.704 \pm 0.87F$. The apparent violation of charge independence exhibited by the scattering length amounts to very little in terms of the strength of a potential. For example, Breit et al. (*36*) find that it represents only a 1.66% difference in the depth of the non-OPEP part of ^1S *np* and a ^1S *pp* potential. Hamada and Johnston state (*38*) that merely reducing their core radius from .343 to .341 gives $a = -23.7F$. Breit, Friedman, Holt, and Seamon (*39*) explore two "speculative" models by which the charged and neutral pion mass difference plus variation of the πN coupling constant might account for apparant violation of charge independence.

An approximate effective range expansion for the case where the Coulomb potential is present is (*40*)

$$C^2k \cot \delta + 2k\eta h(\eta) = -1/a + \tfrac{1}{2}r_e k^2 - Pr_e^3 k^4 \qquad (24)$$

where

$$C^2 = 2\pi\eta/(e^{2\pi\eta} - 1)$$

$$\eta = Me^2/(2\hbar^2 k)$$

$$h(\eta) = -\gamma - \log \eta + \eta^2 \sum_{m=1}^{\infty} [m(m^2 + \eta^2)]^{-1} \quad \text{and} \quad \gamma = .5772 \cdots$$

Using (24) and three low energy ^1S phase shifts the parameters in Table IV were obtained.

The values in Table IV are only approximately correct due principally to our neglect of vacuum polarization effects. Including vacuum polarization Heller (*41*) gets $a = -7.817 \pm .007F$, $r_e = 2.810 \pm .018F$ and $F = .035 \pm .009$.

Our HC, SC and the HJ potentials are plotted in Figs. 1 through 5. Phase shifts obtained from them are given in Figs. 6 through 8. There is no reason for comparing with the HJ rather than the equally good Yale potential.

TABLE IV

^1S EFFECTIVE RANGE PARAMETERS INCLUDING COULOMB EFFECTS

Potential	$a(F)$	$r_e(F)$	P
HC	−7.75	2.78	.024
SC	−7.78	2.72	.028
SCA	−7.77	2.72	.027

Theoretically if a potential is assumed to be local and static, does not have a bound state and must reproduce a phase shift known from $E = 0$ to $E = \infty$, then the potential is uniquely determined. Such theorems do us no good at all for even if the phase were known at very high energies we could not use the nonrelativistic Schrödinger equation there.

The result of fitting phases up to a maximum energy of only 350 MeV is primarily a drastic lack of uniqueness in the short range part. For example, to the accuracy of the plot in Fig. 6 the ^1S phase shifts obtained from the HC, SC, and HJ potentials are the same and agree with the AM and YRB1 values. Yet the corresponding potentials in Fig. 1 are quite different.

Consider two potentials which fit ^1S phases and let their names be A and B. If in some region A is less attractive than B then in general A will be more attractive than B in the two neighboring regions. There is a sort of balancing which goes on. It is most striking inside one Fermi. In order that the ^1S phase be made to go negative above 250 MeV a strong short range repulsion is required. Just outside there is a region of strong attraction and this attraction is greater the more powerful the short range repulsion. Outside $1F$ there can still be fairly large fluctuations. In particular if A is much less attractive than B just inside $1F$ there will be a compensating region outside. This behavior is clearly exhibited by the potentials in Fig. 1. The unplotted alternate soft core model (SCA) is somewhat less repulsive than the soft core (SC) but the SC has a maximum depth of -97 MeV while the SCA only reaches -89 MeV. Outside $1F$ the SC and SCA agree rather closely.

If the SC potential is made only 1% more attractive for $r > 1F$ the fit is destroyed. For example, the phase shift at 1.397 MeV increases by .03 radian (1.7°). This is sixty times the error quoted by Heller (*30*) and ten times larger than changes due to vacuum polarization effects. Even at 50 MeV the phase change of .008 radian (.5°) is greater than the uncertainty in the experimental value. The balancing act is evidently done with considerable care. This result implies that very little information concerning the shapes of potentials tolerated by the data can be gleaned from a single example whose functional form is as simple as ours. In particular for all practical purposes no parameter can by itself be changed at all without significantly altering the phase shifts predicted by the model.

Notice that data obtained from elastic scattering of two nonrelativistic nucleons cannot distinguish between hard and soft cores.

Due to the centrifugal barrier the region of drastic nonuniqueness grows rapidly as the orbital angular momentum increases. This is illustrated by the plot of the two soft core ^1D potentials in Fig. 5. The potentials are dramatically different yet very little of this is reflected in their phase shifts given in Table II. In contrast to the ^1S situation there is no demand by the data for a repulsive core in the ^1D state.

In Fig. 8 one notices that the $^3F_2$ phases appear to differ considerably and that

the HJ $^3P_2$ phase is too large above 150 MeV. Actually, the scale used on the $^3F_2$ plot is large. Since the phase itself is so small the differences are probably not bad. The size of the HJ $^3P_2$ phase is undoubtedly due to the fact that the HJ central potential is considerably less repulsive than the SC and HC models in the region .5 to $1F$ (see Fig. 4).

B. Isotopic Spin Zero

Proton-proton scattering data are more accurate and abundant than *np* data. This is in the nature of things. Protons can be easily accelerated and counted. Neutron beams usually have a larger energy spread and neutron targets require corrections for the protons necessarily present. Since phases for states with isotopic spin zero are extracted from *np* data they are not as well determined as those in the $T = 1$ case.

Hard core $T = 0$ potentials are given in Eqs. (25) through (27). The hard core radius, x_c, is .38383 in the $^3S_1 - {}^3D_1$ state and .3 in the others. It was allowed to vary only in the $^3S_1 - {}^3D_1$ state.

$$V(^1P) = 3h(e^{-x} - 11.08e^{-2x} + 20.3e^{-3x} + 465e^{-6x})/x \tag{25}$$

$$V(^3D_2) = -h(G_3 + 28.45e^{-2x} - 93.6e^{-3x})/x \tag{26}$$

where

$$G_3 = (3 + 6/x + 6/x^2)\, e^{-x} - (18/x + 6/x^2)\, e^{-3x}$$

$$V(^3S_1 - {}^3D_1) = V_C + V_T S_{12} + V_{LS}\mathbf{L}\cdot\mathbf{S} \tag{27}$$

where

$$V_C = -h(e^{-x} + 387.4e^{-6x})/x$$

$$V_T = -h[(1 + 3/x + 3/x^2)\, e^{-x} - (59.968 + 18/x + 3/x^2)\, e^{-6x} - 5.33e^{-3x}]/x$$

$$V_{LS} = 1181.2e^{-6x}/x$$

Again $h = 10.463$ MeV from the OPEP and $x = \mu r$ with $\mu = .7F^{-1}$.

Phase parameters calculated from these potentials are given in Table V.

Soft core $T = 0$ potentials in MeV are given in Eqs. (28) through (30).

$$V(^1P_1) = 3he^{-x}/x - 634.39e^{-2x}/x + 2163.4e^{-3x}/x \tag{28}$$

$$V(^3D_2) = -3h[(1 + 2/x + 2/x^2)\, e^{-x} - (8/x + 2/x^2)\, e^{-4x}]/x - 220.12e^{-2x}/x + 871e^{-3x}/x \tag{29}$$

$$V(^3S_1 - {}^3D_1) = V_C + V_T S_{12} + V_{LS}\mathbf{L}\cdot\mathbf{S} \tag{30}$$

TABLE V

$T = 0$ HARD CORE PHASE PARAMETERS

E	δ ($^1P_1$, radians)		δ ($^3D_2$, radians)	
Lab, MeV	Potential	YLAN (*27*)	Potential	YLAN
19.785	−.053	−.046	.055	.066
47.5	−.104	−.111	.177	.190
105	−.244	−.246	.342	.339
140	−.336	−.328	.388	.381
215	−.521	−.505	.422	.421
300	−.707	−.707	.414	.427
350	−.805	−.827	.401	.421

E	δ ($^3S_1$, radians)		δ ($^3D_1$, radians)		$\rho_1 = \sin(2\epsilon_1)$	
Lab, MeV	Pot.	YLAN	Pot.	YLAN	Pot.	YLAN
19.785	1.515	1.519	−.036	−.034	.057	.053
47.5	1.125	1.130	−.111	−.124	.075	.078
105	.721	.725	−.235	−.226	.105	.103
140	.558	.558	−.291	−.270	.128	.112
215	.293	.281	−.381	−.357	.190	.152
300	.067	.044	−.446	−.444	.270	.244
350	−.044	−.071	−.470	−.493	.320	.311

where

$$V_C = -he^{-x}/x + 105.468^{-2x}/x - 3187.8e^{-4x}/x + 9924.3e^{-6x}/x$$
$$V_T = -h[(1 + 3/x + 3/x^2)\, e^{-x} - (12/x + 3/x^2)\, e^{-4x}]/x + 351.77e^{-4x}/x - 1673.5e^{-6x}/x$$
$$V_{LS} = 708.91e^{-4x}/x - 2713.1e^{-6x}/x$$

Two alternate potentials are

$$V(^3S_1 - {}^3D_1, \text{alternate}) = V_C + V_T S_{12} + V_{LS}\mathbf{L}\cdot\mathbf{S} \qquad (31)$$

where

$$V_C = -he^{-x}/x + 102.012\, e^{-2x}/x - 2915\, e^{-4x}/x + 7800\, e^{-6x}/x$$
$$V_T = -h[(1 + 3/x + 3/x^2)\, e^{-x} - (12/x + 3/x^2)\, e^{-4x}]/x + 163\, e^{-4x}/x$$
$$V_{LS} = 251.57\, e^{-4x}/x$$
$$V(^1P_1, \text{alternate}) = 3he^{-x}/x - 240\, e^{-2x}/x + 17000\, e^{-6x}/x \qquad (32)$$

Phase parameters calculated from these potentials are given in Table VI.

Three low energy $^3S_1$ phase shifts were used to calculate the parameters in Table VII from the effective range expansion (23). Analyzing *np* data Noyes (*35*) finds $a = 5.396 \pm .011F$ $r_e = 1.726 \pm .014F$. Houk and Wilson (*37*) obtain $a = 5.425 \pm .004F$ and $r_e = 1.749 \pm .008$. P is not well determined by the data.

TABLE VI

$T = 0$ SOFT CORE PHASE PARAMETERS

E	δ ($^1P_1$, radians)			δ ($^3D_2$, radians)		
Lab, MeV	Potential	A–M (*28*)	Alternate Potential	Potential	A–M	
24	−.033	−.041	−.060	.070	.071	
48	−.071	−.072	−.094	.169	.169	
96	−.190	−.182	−.188	.312	.309	
144	−.312	−.309	−.299	.386	.386	
208	−.456	−.463	−.448	.431	.433	
304	−.633	−.646	−.651	.449	.451	
352	−.708	−.717	−.744	.448	.449	

E	δ ($^3S_1$, radians)			δ ($^3D_1$, radians)		
	Pot.	A–M	Alternate Potential	Pot.	A–M	Alternate Potential
24	1.426	1.443	1.426	−.050	−.051	−.050
48	1.105	1.138	1.106	−.115	−.123	−.117
96	.749	.771	.750	−.215	−.218	−.220
144	.521	.513	.523	−.281	−.272	−.288
208	.300	.269	.305	−.340	−.329	−.345
304	.057	.066	.068	−.403	−.432	−.387
352	−.042	.020	−.027	−.431	−.494	−.399

E	$\rho_1 = \sin(2\epsilon_1)$		
Lab, MeV	Pot.	A–M	Alternate Potential
24	.064	−.042	.060
48	.081	−.102	.073
96	.114	−.055	.098
144	.152	.064	.131
208	.203	.212	.183
304	.269	.368	.267
352	.296	.422	.307

TABLE VII

^3S EFFECTIVE RANGE PARAMETERS

Potential	$a(F)$	$r_e(F)$	P
HC	5.397	1.724	−.011
SC	5.390	1.720	−.027
SCA	5.390	1.720	−.027

TABLE VIII

PROPERTIES OF THE DEUTERON

Potential	E (MeV)	Q (F^2)	P_D (%)	A_D/A_S
HC	2.22464	.2770	6.497	.02590
SC	2.22460	.2796	6.470	.02622
SCA	2.22464	.2762	6.217	.02596

Properties of the deuteron calculated from our potentials are given in Table VIII where E is the binding energy, Q is the electric quadrupole moment, P_D is the D-state probability and A_D/A_S is the asymptotic D to S wave ratio. Experimentally $E = 2.22462 \pm .00006$ MeV (*42*). The potential of Hamada and Johnson (*11*) gives $E = 2.269$ MeV not the value 2.226 MeV, which they quote.

The quantity Qq, where q is the gradient of the electric field of the D_2 molecule taken along the molecular axis and evaluated at one of the two deuterons, has been measured to one part in 6000 (*43*). Although q cannot be obtained experimentally it can be calculated from the D_2 molecular wave function. Newell (*44*) found a wave function, calculated q and estimated his error to be .6%. Newell's q yields (*43*) $Q = .2738 \pm .0014F^2$. More recently, Auffray (*45*) obtained a better wave function, calculated q and found $Q = .282$. The superiority of his wave function rests on the grounds that his energy eigenvalue differs from experiment by .4%, while Newell's differs by 3.8%. However, variational wavefunctions yielding about the same energy can differ greatly in their predictions for other quantities. Lomon and Feshbach (*14*), (*15*) take $Q = .278 \pm .008F^2$. We conclude that our potentials yield Q's well within the accuracy to which this quantity is known.

Bethe (*46*) estimated P_D to be between 2% and 8%. It has not been accurately determined experimentally.

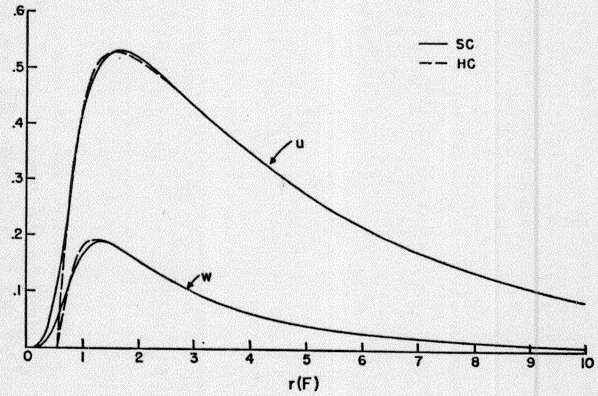

FIG. 9. Soft core (SC) and hard core (HC) deuteron wave functions.

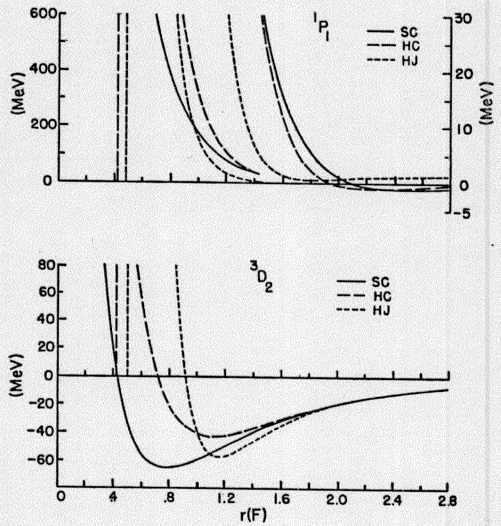

FIG. 10. Soft core (SC), hard core (HC) and Hamada–Johnston (HJ) $^1P_1$ and $^3D_2$ potentials. In the $^1P_1$ graph the rightmost curves correspond to the scale on the right side.

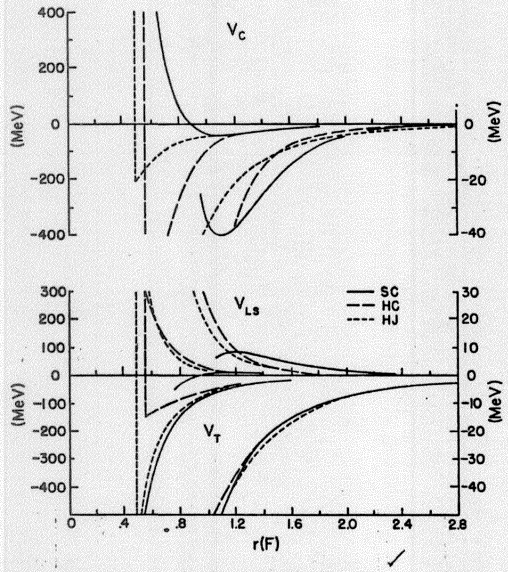

FIG. 11. Soft core (SC), hard core (HC) and Hamada–Johnston (HJ) $^3S_1$–$^3D_1$ potentials. The HJ V_{LL} has been put into their V_{LS}. Note that the SC V_{LS} is negative for $r < .95F$.

Deuteron wave functions are plotted in Fig. 9. They are described and tabulated in the Appendix. Our HC, SC and the HJ potentials are plotted in Figs. 10 through 12. Their phase shifts are given in Figs. 13 through 15.

The difference between our SC and HC $^1P_1$ potentials seen in Fig. 10 is responsible for the disagreement in their phase shifts evident in Fig. 13 and is largely due to differences in the phases to which the two potentials were fit. That the $^1P_1$ phase shift is experimentally poorly determined by existing scattering data is immediately obvious from Table IX.[7]

Except for the SC $^1P_1$, the OPEP is the dominant part of all our potentials for $r > 3F$. The non-OPEP (OPEP) part of the SC $^1P_1$ model is -2.64 (1.83) MeV at $r = 3F$ and $-.66$ (.68) at $4F$. This deviation from the OPEP may make the alternate soft core potential slightly preferable.

The D-wave centrifugal barrier is large enough for very little of the differences

[7] The point we wish to make is not that the data tolerate any $^1P_1$ phase shift, but that phases which would correspond to quite different potentials are not violently rejected. The OPEP alone gives $\delta = -.156$ radians at 48 MeV and $-.225$ at 352 MeV.

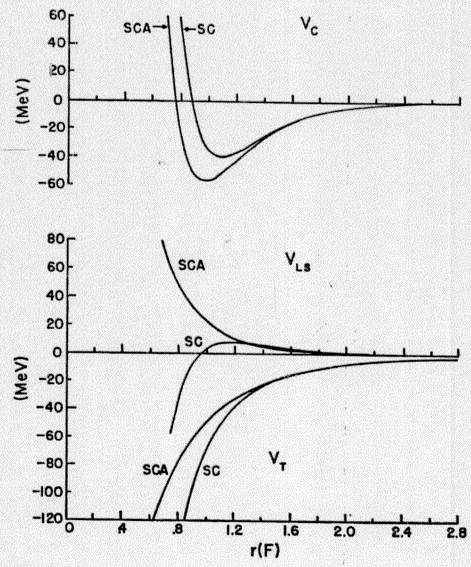

FIG. 12. Comparison of the soft core (SC) and alternate soft core (SCA) $^3S_1$–$^3D_1$ potentials.

in the $^3D_2$ potentials seen in Fig. 10 to be exhibited by their phase shifts plotted in Fig. 13. Recall that the same effect was observed in the $^1D_2$ state; see Fig. 5 and Table II.

In the $^3S_1 - {}^3D_1$ state there are three functions of r, $V_C(r)$, $V_T(r)$ and $V_{LS}(r)$, to be determined by three energy dependent phase parameters, $\delta(^3S_1)$, $\delta(^3D_1)$ and $\rho_1 = \sin(2\epsilon_1)$. However, Table X and the work of Simmons (*49*) make it

TABLE IX

$^1P_1$ PHASE SHIFTS FROM RECENT ENERGY DEPENDENT ANALYSES

Search	δ (48 MeV, radians)	δ (352 MeV, radians)
AM (*24*)	−.055	−.717
AM (*28*)	−.072	−.717
AM (*47*)	−.037	−.560
Yale (*48*)	−.120	−.779

clear that experimentally ρ_1 is very poorly known. This has particularly woeful implications for our knowledge of the tensor force since ρ_1 even owes its existence to a nonzero V_T. In addition, it is possible, without substantially changing

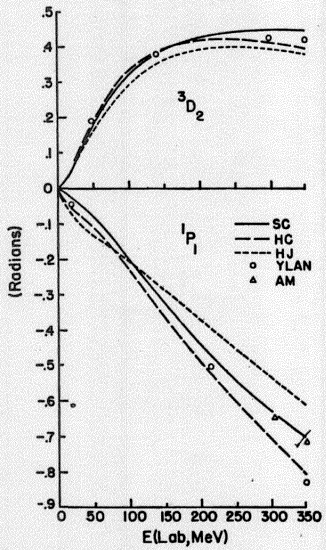

FIG. 13. Soft core (SC), hard core (HC) and Hamada–Johnston (HJ) $^1P_1$ and $^3D_2$ phase shifts. The HJ phases are taken from their paper (*11*). Yale YLAN4MP (*27*) phases are plotted only when they differ significantly from those of the HC and the Arndt and MacGregor (AM) (*28*) when they differ from the SC.

TABLE X

VALUES OF ρ_1 FROM RECENT ENERGY DEPENDENT ANALYSES

Search	ρ_1 (48 MeV)	ρ_1 (352 MeV)
AM (*24*)	.123	.665
AM (*28*)	−.102	.422
AM (*47*)	−.083	.264
Yale (*48*)	.078	.217

predicted phase parameters, to make V_C considerably less attractive provided that V_T is made more negative at the same time, and vice versa. This ambiguity in the central-to-tensor ratio can be seen in Figs. 12 and 15 where the SC and SCA potentials and their phase parameters are compared. Finally there is the usual uncertainty in the short range behavior of the potentials arising from a restriction to an upper limit on the energy of about 350 MeV.

Notice that except for the short range part of the SC model, V_{LS} has a sign opposite to that in the $^3P_2 - {}^3F_2$ state. This is in agreement with the Yale and HJ potentials. V_{LS} is also clearly less well determined and apparently weaker than that in the $^3P_2 - {}^3F_2$ state.

One of the most striking features of the $^3S_1 - {}^3D_1$ potential is that it has a bound state, the deuteron, in spite of the weakness of the attraction in the central potential, $V_C(r)$. Compare the SC V_C in Fig. 11 with the SC $^1S_0$ potential in Fig. 1

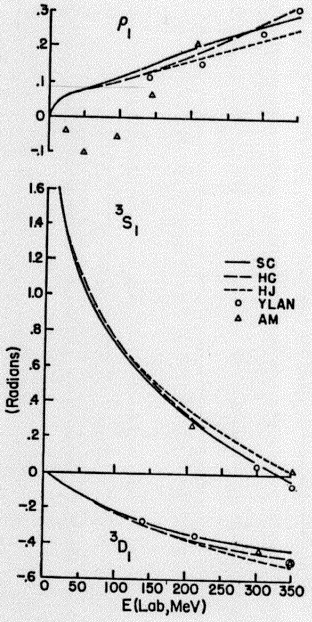

FIG. 14. $^3S_1$–$^3D_1$ phase parameters. See caption to Fig. 13. The AM values for ρ_1 at 304 and 352 MeV are not plotted.

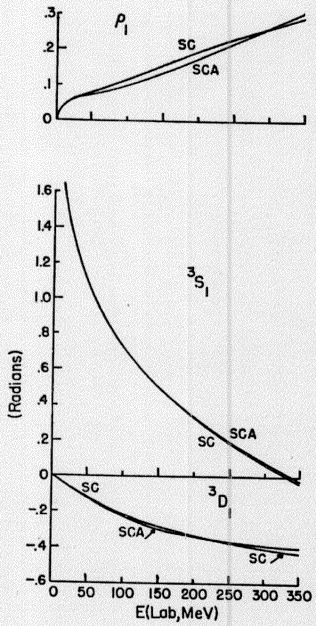

FIG. 15. Comparison of the soft core (SC) and alternate soft core (SCA) $^3S_1$–$^3D_1$ phase parameters.

and bear in mind the non-existence of a bound $^1S_0$ state.[8] Indeed the S-wave phase shift calculated from the SC central potential with no coupling to the D-state has a maximum of only .1 radian (5.7°) at about 10 MeV and turns negative at 48 MeV. A large part of the attraction present in the $^3S_1 - {}^3D_1$ state is a direct consequence of the tensor coupling.

IV. VELOCITY DEPENDENCE OF LOCAL POTENTIALS

If the NN potential depends at most linearly on the relative momentum then (*8*) a single central potential, $V(r)$, must act in all (spin) singlet-odd (parity) states and one other in all singlet even. Moreover, all the triplet-odd states must be described by a single potential of the form

$$V = V_C(r) + V_T(r)\, S_{12} + V_{LS}(r)\, \mathbf{L}\cdot\mathbf{S} \tag{33}$$

and another of the same form must characterize all triplet-even states simultaneously.

From the $^1P_1$ phase shifts in Table IX and Fig. 13 we conclude that forces in singlet-odd states are so poorly determined by available scattering data that the question of whether or not a single $V(r)$ will suffice must remain unanswered at present.

The singlet-even states are quite another matter for their phase shifts are among the best known. A static and local potential which is fit to $^1S_0$ phases gives $^1D_2$ phases which are too large at high energies. The magnitude of the problem can be seen in Table XI and Fig. 16.

TABLE XI

$^1D_2$ PHASE SHIFTS CALCULATED FROM $^1S_0$ POTENTIALS

E	$\delta(^1D_2$, radians) from potentials				$\delta(^1D_2$, radians)
Lab, MeV	HC	SC	SCA	HJ	AM (*51*)
48	.032	.029	.029	.031	.029 ± .003
96	.077	.072	.072	.073	.061 ± .003
208	.183	.183	.185	.176	.120 ± .003
352	.281	.286	.285	.287	.176 ± .010

[8] For an interesting comparison of a ^1S potential with a ^3S central which does have a bound state, see Coester and Yen (*50*).

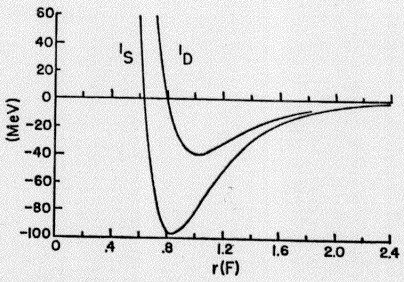

FIG. 16. Comparison of the soft core $^1S_0$ and $^1D_2$ potentials.

There have been many attempts to solve this problem. In 1957, Gammel and Thaler (*52*) found that static and local $^1S_0$ potentials which fit the scattering length, effective range and the 310 MeV $^1S_0$ phase shift give a $^1D_2$ phase of about .26 at 310 MeV. In 1960 they stated (*53*) that the value, .26, could be reduced to

TABLE XII

TRIPLET-ODD PHASE PARAMETERS CALCULATED FROM THE SOFT CORE $^3P_2$–$^3F_2$ POTENTIAL

E	$\delta(^3P_0$, radians)		$\delta(^3P_1$, radians)		$\delta(^3F_3$, radians)	
Lab, MeV	SC	AM (*51*)	SC	AM	SC	AM
24	.148	.122 ± .005	−.081	−.074 ± .004	−.004	−.004
48	.211	.213 ± .007	−.136	−.132 ± .004	−.011	−.012 ± .001
96	.203	.186 ± .009	−.214	−.228 ± .005	−.026	−.027 ± .002
144	.140	.099 ± .010	−.278	−.306 ± .006	−.038	−.039 ± .003
208	.040	−.009 ± .010	−.357	−.387 ± .007	−.049	−.048 ± .003
304	−.109	−.173 ± .022	−.467	−.477 ± .013	−.062	−.054 ± .006
352	−.178	−.273 ± .035	−.519	−.514 ± .017	−.068	−.056 ± .009

	$\delta(^3F_4$, radians)		$\rho_4 = \sin(2\epsilon_4)$		$\delta(^3H_4$, radians)	
	SC	AM	SC	AM	SC	AM
48	.002	.003	−.006	−.006	.0004	.0005
96	.007	.010 ± .002	−.018	−.018 ± .001	.002	.002
144	.016	.020 ± .002	−.028	−.027 ± .002	.003	.005 ± .001
208	.033	.034 ± .002	−.040	−.033 ± .002	.006	.009 ± .002
304	.070	.054 ± .004	−.052	−.032 ± .008	.009	.016 ± .005
352	.093	.063 ± .006	−.056	−.028 ± .010	.010	.019 ± .006

about .225 by using a potential which has two attractive regions, one of very long range. They pointed out, however, that this shape gives unreasonably large $^1G_4$ phases. Hamada (*54*) found that large $^1D_2$ phases give too large a forward peak in the differential cross section at high energies and added a quadratic spin-orbit term (see Eq. 7a) to the singlet-even potential. Lee, Gammel and Thaler (*55*) and later Giltinan and Thaler (*56*) used non-local potentials to depress the D phases. In 1961, Yoder and Signell (*57*) tried to make a single central potential fit ^1S and ^1D phases at 95 and 310 MeV and the scattering length and effective range. They found it difficult despite the fact that the $^1D_2$ phase at 310 MeV was allowed to be as large as .25 radian. This value is not much below that predicted by the $^1S_0$ potentials in Table XI and is much larger than more recent experiments indicate. Yoder and Signell reject their potential on the grounds that it did not go over into the OPEP fast enough at large r. For example, it was +.5 MeV at 2.8 Fermis while the OPEP is −.75 MeV there. In 1965, Noyes (*58*) fit a soft (Yukawa) core potential to $^1S_0$ phase shifts and compared its predictions for $^1D_2$ and $^1G_4$ phases with those of the hard core $^1S_0$ potential of Heller, Signell and Yoder (*33*) and with Livermore phases extracted from scattering data. He found that the hard and soft core models agree closely in the D and G states, that their phases were much too large and concludes that nonlocal and/or nonstatic effects are being seen in the singlet-even states. The $^1S_0$ potential predictions for D phases gives by Noyes are essentially the same as those in Table XI.

The inability of a single local potential $V(r)$, to describe all singlet-even states simultaneously is not hard to understand. By itself the part of a ^1S potential for $r > 1F$ is too attractive in the ^1D state. For example this part of our SC model gives a ^1D phase of .226 at 304 MeV. Only a very small amount of this attraction can be moved to larger r without disrupting low energy ^1D phases and broadening the 10 MeV ^1S phase shift peak. Shifting attraction to smaller r would appear appealing due to the centrifugal barrier in the D-state (see Fig. 5) but this too, doesn't work. An increase in short range attraction makes high-E ^1S phases too large unless the core is made more repulsive. But a more repulsive core in turn demands yet more attraction to regain a fit to low-E ^1S phases. The D-wave centrifugal barrier cannot hide all that attraction and high-E ^1D phases are almost unchanged by the entire process. Thus failure to fit all singlet-even states simultaneously is inevitable.

Of course, there exist infinitely many velocity-dependent and/or nonlocal models which can reproduce singlet-even phase parameters. Lomon and Feshbach (*14*), (*15*) make their boundary condition L-dependent, out choice of different local potentials for each state has implied velocity-dependence, and the form of HJ or Yale (see Eq. 7a) uses two independent local potentials for the three lowest angular momentum states and the OPEP after that.

Phase parameters in the triplet-odd states are fairly well determined. We looked

to see whether a single potential of the form (33) would reproduce $^3P_0$, $^3P_1$, $^3F_3$, $^3P_2 - {}^3F_2$ and $^3F_4 - {}^3H_4$ phases. It failed by a substantial margin. However, qualitative fits are astonishingly easy to obtain. This is illustrated in Table XII where predictions of our soft core $^3P_2 - {}^3F_2$ model for the other states are compared with results of Arndt and MacGregor. The state whose phases are the most difficult to reconcile with the others is the $^3F_4 - {}^3H_4$, where poor high energy behavior of the phases is caused chiefly by the powerful negative V_{LS} plotted in Fig. 4. From Eq. (9) one sees that V_{LS} is attractive with a coefficient 3 in the $^3F_4$ equation and repulsive with a coefficient 6 in the $^3H_4$. Yet V_{LS} could scarcely be weakened for in the $^3P_0$ state it is repulsive with a coefficient 2 and the $^3P_0$ phase in Table XII exhibits a need for greater short range repulsion.

The Yale potential uses (33) in triplet-odd states, and the HJ model has the same form as far as the $^3P_2 - {}^3F_2$ and $^3F_4 - {}^3H_4$ states are concerned. The HJ potential has $^3F_4$ phases which are too large at high energies. Hamada and Johnston remark that this results in a bump in the *pp* differential cross section which is not present in the data. The Yale potential solves the problem by putting $V_{LS} = 0$ for $J > 2$. Tamagaki and Watari (*59*) recommend adding a second quadratic spin-orbit potential to the HJ form.

The most striking obstacle to describing all triplet-even states with one potential of the form (33) is the high energy behavior of the $^3D_2$ phase shift. In 1960 Hamada (*60*) fit potentials of the form $V = V_C(r) + V_T(r)\,S_{12}$ to low energy $^3S_1 - {}^3D_1$ data. Shortly afterwards (*61*) he noticed that all of his potentials predicted values for the $^3D_2$ phase which at high energies are so large (>.78 radian at 300 MeV) that serious disagreement with experimental *np* total cross section occurs. Later (*62*) he attributed the difficulty to the fact that low energy $^3S_1 - {}^3D_1$ data require a V_T which is like the OPEP for $x > 1$.

Both the Yale the HJ potentials employ a quadratic spin-orbit term here largely to depress the $^3D_2$ phase shift. Without it the Yale group found (*12*) that reasonable potentials predict high energy values greater than about .7 radian. The quadratic

TABLE XIII

$^3D_2$ PHASE SHIFTS PREDICTED BY $^3S_1$–$^3D_1$ POTENTIALS

E	δ ($^3D_2$, radians) from potentials			δ ($^3D_2$, radians)
Lab, MeV	HC	SC	SCA	AM (*63*)
24	.064	.061	.061	.071 ± .004
96	.365	.370	.365	.309 ± .012
352	.999	.895	.916	.449 ± .045

spin-orbit term of Hamada and Johnston reduces $\delta(^3D_2)$ at 300 MeV from .819 to .397.

A potential of the form (33) is

$$V(^3D_2) = V_C(r) + 2V_T(r) - V_{LS}(r) \tag{34}$$

in the $^3D_2$ state. Table XIII contains $^3D_2$ phase shifts predicted in this manner by our $^3S_1 - {}^3D_1$ potentials.

From Figs. 11 and 12 and Eq. (34) it is clear that in general all parts, V_C, V_T, and V_{LS} of the $^3S_1 - {}^3D_1$ potentials tend to increase the $^3D_2$ phase. However, V_T appears with a factor of 2. Its behavior is crucial. Doubling the V_T in Figs. 11 and 12 and comparing with the $^3D_2$ potentials in Fig. 10 one sees that it alone will give too much attraction in the $^3D_2$ state. What is apparently needed is a large shift in attraction from V_T to V_C.

We took the soft core $^3S_1 - {}^3D_1$ model, halved V_T and did *not* change V_C or V_{LS}. The resulting $^3D_2$ phase at 352 MeV was .550 radian. This is still too large and it would rise by a considerable amount if V_C were made more attractive to, say, again bind the deuteron at the proper energy. Moreover we added a e^{-2x}/x Yukawa to the V_T of both the SC and SCA $^3S_1 - {}^3D_1$ potentials and tried to weaken the tail of V_T while retaining a fit in the $^3S_1 - {}^3D_1$ state. In agreement with Hamada we were unable to drastically alter V_T outside $x = 1$. Thus it is probably impossible to halve V_T yet even that is not nearly enough to achieve a simultaneous fit in the $^3S_1 - {}^3D_1$ and $^3D_2$ states.

V. CONCLUSIONS

Considerable velocity-dependence and/or nonlocality of the *NN* potential is clearly required by scattering data. A local potential which is at most linear in the relative momentum, **p**, is definitely excluded. One with a p^2 dependence of the HJ or Yale type is probably also excluded, but its failures are not likely to significantly affect the results of present-day calculations which use *NN* potentials.

The complicated nature of the interaction has the unfortunate consequence that, for example, it is only approximately correct to speak of *the* triplet-odd spin-orbit force or *the* singlet-even repulsive core, except within the context of an adequate model.

Except for the ρ_1 resulting from some analyses, accurate fits to phase parameters can be obtained with simple potentials. In $T = 1$ states the phase parameters are so well determined by scattering data that, once an adequate model is chosen, the uncertainties in the corresponding potentials are largely due to the necessity of working below an upper energy limit of about 350 MeV. $T = 0$ phase parameters are in a much less satisfactory condition. Both the crucial $^3S_1 - {}^3D_1$ and the important $^1P_1$ phase parameters are only crudely determined by available *np* data.

ACKNOWLEDGMENTS

Particular thanks are due to Professor H. A. Bethe for helpful suggestions throughout the course of this work. We are also indebted to Professors Gregory Breit and Richard Arndt for information related to nucleon-nucleon phase parameters; to Professor H. P. Noyes for communications and discussions regarding nonlocal and/or nonstatic effects in the singlet-even states; to Dr. Michael Kirson for many helpful discussions; to Professor Mario Iona for general advice; to Professors Breit, K. A. Friedman and R. E. Seamon, Dr. R. D. Haracz, and J. M. Holt for checking the numerical accuracy of phase parameters from the soft core potentials; to Professors Peter Signell and N. R. Yoder for checking the fit of our hard core potential to *pp* scattering data, and to Professors E. L. Lomon and A. K. Kerman for critically reading the manuscript.

APPENDIX. WAVEFUNCTIONS OF THE DEUTERON

Properties of the deuteron were calculated using the approach of Hamada (*60*) except that where he integrates solely inward we followed a suggestion of Sprung (*64*), and also integrated outward from near the origin to a convenient matching point such as $1.5F$. Sprung's approach is numerically the most stable.

For the purpose of obtaining deuteron wave functions the hard core $^3S_1 - {}^3D_1$ potential was assumed to vanish beyond $x_p = 10.38383$ and the soft core beyond $x_p = 10.01$. In addition, a convenient but fictitious hard core of radius $x_c = .01$ was used with the soft core model. If no fictitious hard core is used with the soft core potential then $u \sim r$ and $w \sim r^2$ as $r \to 0$. For $x \geqslant x_p$ the wave functions are

$$\begin{aligned} u &= A_S e^{-\alpha x} \\ w &= A_S(A_D/A_S)\, e^{-\alpha x}[1 + 3/(\alpha x) + 3/(\alpha x)^2] \end{aligned} \tag{A.1}$$

TABLE XIV

CONSTANTS FOR DEUTERON WAVE FUNCTIONS

	Potential	
Constant	HC	SC
α	.33088	.33087
A_S	.88034	.87758
A_D/A_S	.025900	.026223
Q (F^2)	.27700	.27964
P_D (%)	6.4970	6.4696

where

$$\alpha = (ME)^{1/2}/(\mu\hbar)$$

As usual $x = \mu r$ with $\mu = .7F^{-1}$ and $\hbar^2/M = 41.47$ MeV F^2. The normalization is

$$\frac{1}{\mu}\int_0^\infty (u^2 + w^2)\, dx = 1. \qquad \text{(A.2)}$$

Other constants are given in Table XIV. For $x < x_p$ the wave functions are plotted in Fig. 9 and given in Tables XV and XVI.

TABLE XV

HARD CORE DEUTERON WAVE FUNCTIONS[a]

x	u	w	du/dx	dw/dx
3.83830 −1	0.0	0.0	2.0955 0	9.9834 −1
4.46330 −1	1.2676 −1	5.9692 −2	1.9096 0	8.7978 −1
5.08830 −1	2.3528 −1	1.0804 −1	1.5532 0	6.6347 −1
5.71330 −1	3.2091 −1	1.4290 −1	1.1929 0	4.5773 −1
6.33830 −1	3.8556 −1	1.6615 −1	8.8655 −1	2.9380 −1
7.58830 −1	4.6726 −1	1.8845 −1	4.5852 −1	8.6198 −2
8.83830 −1	5.0777 −1	1.9205 −1	2.1270 −1	−1.6172 −2
1.00883 0	5.2478 −1	1.8663 −1	7.2431 −2	−6.4401 −2
1.13383 0	5.2827 −1	1.7705 −1	−9.4837 −3	−8.5724 −2
1.25883 0	5.2376 −1	1.6575 −1	−5.8600 −2	−9.3469 −2
1.38383 0	5.1441 −1	1.5397 −1	−8.8563 −2	−9.4204 −2
1.63383 0	4.8801 −1	1.3123 −1	−1.1775 −1	−8.6506 −2
1.88383 0	4.5719 −1	1.1102 −1	−1.2664 −1	−7.4923 −2
2.38383 0	3.9435 −1	7.9259 −2	−1.2186 −1	−5.2933 −2
2.88383 0	3.3672 −1	5.7106 −2	−1.0813 −1	−3.6652 −2
3.38383 0	2.8636 −1	4.1749 −2	−9.3419 −2	−2.5501 −2
3.88383 0	2.4310 −1	3.1002 −2	−7.9874 −2	−1.7982 −2
4.38383 0	2.0620 −1	2.3366 −2	−6.7984 −2	−1.2886 −2
4.88383 0	1.7484 −1	1.7851 −2	−5.7741 −2	−9.3889 −3
5.38383 0	1.4821 −1	1.3802 −2	−4.8991 −2	−6.9500 −3
5.88383 0	1.2563 −1	1.0783 −2	−4.1545 −2	−5.2202 −3
6.38383 0	1.0648 −1	8.5013 −3	−3.5221 −2	−3.9728 −3
7.38383 0	7.6489 −2	5.4035 −3	−2.5306 −2	−2.3795 −3
8.38383 0	5.4943 −2	3.5156 −3	−1.8179 −2	−1.4775 −3
9.38383 0	3.9465 −2	2.3277 −3	−1.3058 −2	−9.4290 −4

[a] Each entry is followed by its exponent to the base 10.

TABLE XVI

SOFT CORE DEUTERON WAVE FUNCTIONS[a]

x	u	w	du/dx	dw/dx
1.000 −2	0.0	0.0	2.9751 −4	7.4202 −5
4.125 −2	3.3373 −5	1.0850 −5	2.6127 −3	8.9321 −4
7.250 −2	2.3901 −4	8.4073 −5	1.2335 −2	4.4755 −3
1.350 −1	2.7621 −3	1.0369 −3	8.2951 −2	3.1892 −2
1.975 −1	1.2737 −2	4.9642 −3	2.5326 −1	1.0121 −1
2.600 −1	3.6062 −2	1.4446 −2	5.0052 −1	2.0596 −1
3.225 −1	7.5359 −2	3.0795 −2	7.5072 −1	3.1477 −1
3.850 −1	1.2847 −1	5.3157 −2	9.3349 −1	3.9371 −1
4.475 −1	1.8993 −1	7.8995 −2	1.0162 0	4.2466 −1
5.100 −1	2.5349 −1	1.0525 −1	1.0034 0	4.0842 −1
5.725 −1	3.1390 −1	1.2933 −1	9.2042 −1	3.5772 −1
6.350 −1	3.6770 −1	1.4958 −1	7.9674 −1	2.8848 −1
6.975 −1	4.1317 −1	1.6529 −1	6.5744 −1	2.1428 −1
7.600 −1	4.4992 −1	1.7645 −1	5.1985 −1	1.4427 −1
8.850 −1	4.9953 −1	1.8710 −1	2.8494 −1	3.3294 −2
1.010 0	5.2406 −1	1.8654 −1	1.1865 −1	−3.5899 −2
1.135 0	5.3166 −1	1.7946 −1	1.1397 −2	−7.3151 −2
1.260 0	5.2864 −1	1.6910 −1	−5.4090 −2	−9.0091 −2
1.385 0	5.1926 −1	1.5742 −1	−9.2523 −2	−9.5299 −2
1.510 0	5.0621 −1	1.4553 −1	−1.1418 −1	−9.4158 −2
1.760 0	4.7505 −1	1.2314 −1	−1.3097 −1	−8.3973 −2
2.010 0	4.4200 −1	1.0373 −1	−1.3193 −1	−7.1282 −2
2.510 0	3.7864 −1	7.3859 −2	−1.2004 −1	−4.9327 −2
3.010 0	3.2249 −1	5.3293 −2	−1.0453 −1	−3.3940 −2
3.510 0	2.7399 −1	3.9077 −2	−8.9709 −2	−2.3612 −2
4.010 0	2.3251 −1	2.9115 −2	−7.6510 −2	−1.6691 −2
4.510 0	1.9719 −1	2.2016 −2	−6.5054 −2	−1.2002 −2
5.010 0	1.6718 −1	1.6871 −2	−5.5229 −2	−8.7768 −3
5.510 0	1.4172 −1	1.3079 −2	−4.6850 −2	−6.5201 −3
6.010 0	1.2012 −1	1.0243 −2	−3.9726 −2	−4.9136 −3
7.010 0	8.6290 −2	6.4412 −3	−2.8547 −2	−2.8956 −3
8.010 0	6.1983 −2	4.1575 −3	−2.0508 −2	−1.7758 −3
9.010 0	4.4523 −2	2.7363 −3	−1.4731 −2	−1.1227 −3

[a] Each entry is followed by its exponent to the base 10.

An interpolation formula which is convenient to use with the tabulated deuteron wave function is

$$f(x+ph) = A_1 + A_2 p + A_3 p^2 + A_4 p^3$$
$$\left.\frac{df}{dx}\right|_{x+ph} = f'(x+ph) = A_5 + A_6 p + A_7 p^2 \qquad \text{(A.3)}$$

where

$$0 \leqslant p \leqslant 1$$

$$A_1 = f(x)$$
$$A_2 = hf'(x)$$
$$A_3 = 3[f(x+h) - f(x)] - [2f'(x) + f'(x+h)]\,h$$
$$A_4 = 2[f(x) - f(x+h)] + [f'(x) + f'(x+h)]\,h$$
$$A_5 = f'(x)$$
$$A_6 = 2A_3/h$$
$$A_7 = 3A_4/h$$

RECEIVED: August 23, 1968

REFERENCES

1. J. M. B. KELLOGG, I. I. RABI, N. F. RAMSEY, JR., AND J. R. ZACHARIAS, *Phys. Rev.* **55**, 318 (1939) and *Phys. Rev.* **57**, 677 (1940).
2. H. A. BETHE, *Phys. Rev.* **76**, 38 (1949). See also J. M. BLATT AND J. D. JACKSON, *Phys. Rev.* **76**, 18 (1949).
3. C. R. SCHUMACHER AND H. A. BETHE, *Phys. Rev.* **121**, 1534 (1961).
4. H. A. BETHE, *Scientific American* **189**, 58 (1953).
5. H. P. STAPP, T. J. YPSILANTIS, AND N. METROPOLIS, *Phys. Rev.* **105**, 302 (1957).
6. J. L. GAMMEL, R. S. CHRISTIAN, AND R. M. THALER, *Phys. Rev.* **105**, 311 (1957).
7. J. L. GAMMEL AND R. M. THALER, *Prog. Elem. Particle and Cosmic Ray Phys.* **5**, 99 (1960).
8. L. EISENBUD AND E. WIGNER, *Proc. Nat'l. Acad. Sci. U.S.* **27**, 281 (1941).
9. J. L. GAMMEL AND R. M. THALER, *Phys. Rev.* **107**, 291 and 1337 (1957).
10. P. SIGNELL AND R. E. MARSHAK, *Phys. Rev.* **106**, 832 (1957) and *Phys. Rev.* **109**, 1229 (1958).
11. T. HAMADA AND I. D. JOHNSTON, *Nucl. Phys.* **34**, 382 (1962); T. HAMADA, Y. NAKAMURA AND R. TAMAGAKI, *Prog. Theoret. Phys.* (*Kyoto*) **33**, 769 (1965).
12. K. E. LASSILA, M. H. HULL, JR., H. M. RUPPEL, F. A. MCDONALD AND G. BREIT, *Phys. Rev.* **126**, 881 (1962). (See the first two papers of Ref. (*16*) for phase shifts calculated from the Yale potential).
13. International Conference on the Nucleon–Nucleon Interaction (A. E. S. Green, M. H. MacGregor, and R. Wilson, Eds.), *Rev. Mod. Phys.* **39**, 495–717 (1967).
14. E. L. LOMON AND H. FESHBACH, Reference (*13*), p. 611.
15. E. L. LOMON AND H. FESHBACH, *Ann. Phys.* To be published.

16. G. BREIT, M. H. HULL, JR., K. E. LASSILA, K. D. PYATT, JR., AND H. M. RUPPEL, *Phys. Rev.* **128**, 826 (1962); M. H. HULL, JR., K. E. LASSILA, H. M. RUPPEL, F. A. MCDONALD, AND G. BREIT, *Phys. Rev.* **128**, 830 (1962); G. BREIT, Reference (*13*), p. 560; R. E. SEAMON, K. A. FRIEDMAN, G. BREIT, R. D. HARACZ, J. M. HOLT AND A. PRAKASH, *Phys. Rev.* **165**, 1579 (1968); G. BREIT AND R. D. HARACZ, "High Energy Physics" (E. H. S. Burhop, Ed.), Vol. I, p. 21. Academic Press, Inc., New York, 1967.
17. M. H. MACGREGOR AND R. A. ARNDT, *Phys. Rev.* **139**, B362 (1965); H. P. NOYES, D. S. BAILEY, R. A. ARNDT, AND M. H. MACGREGOR, *Phys. Rev.* **139**, B380 (1965); R. A. ARNDT AND M. H. MACGREGOR, *Phys. Rev.* **141**, 873 (1966); M. H. MACGREGOR, Reference (*13*), p. 556; M. H. MACGREGOR, R. A. ARNDT, AND R. M. WRIGHT, *Phys. Rev.* **169**, 1128 (1968).
18. P. SIGNELL, *Phys. Rev.* **139**, B315 (1965) and references cited there.
19. P. CZIFFRA, M. H. MACGREGOR, M. J. MORAVCSIK, AND H. P. STAPP, *Phys. Rev.* **114**, 880 (1959).
20. G. BREIT, *Rev. Mod. Phys.* **34**, 766 (1962). (See also the last article of Reference (*16*).
21. S. OKUBO AND R. E. MARSHAK, *Ann. Phys.* **4**, 166 (1958).
22. J. L. GAMMEL AND R. M. THALER, Reference (*7*), p. 114.
23. N. FUKUDA AND R. G. NEWTON, *Phys. Rev.* **103**, 1558 (1956); W. B. RIESENFELD AND K. M. WATSON, *Phys. Rev.* **104**, 492 (1956); J. P. ELLIOTT, H. A. MAVROMATIS, AND E. A. SANDERSON, *Phys. Letters* **24B**, 358 (1967).
24. R. A. ARNDT AND M. H. MACGREGOR, *Phys. Rev.* **141**, 873 (1966).
25. C. BRESSEL, A. KERMAN, AND E. LOMON, *Bull. Am. Phys. Soc.* **10**, 584 (1965).
26. C. BRESSEL, A. KERMAN, AND B. ROUBEN, To be published.
27. A. N. CHRISTAKIS, G. BREIT, M. H. HULL, JR., H. M. RUPPEL, AND R. E. SEAMON, Unpublished. See Reference (*16*) for results of more recent phase shift analyses by the Yale group.
28. R. A. ARNDT AND M. H. MACGREGOR, private communication. The $T = 0$ phases of Reference (*24*) were abandoned because some of them are almost certainly wrong below 50 MeV.
29. N. R. YODER AND P. SIGNELL, *Bull. Am. Phys. Soc.* **12**, 50 (1967).
30. L. HELLER, Reference (*13*), p. 584.
31. H. A. BETHE AND P. M. MORRISON, "Elementary Nuclear Theory", 2nd Ed., p. 57. John Wiley and Sons, New York, 1956.
32. I. SLAUS, Reference (*13*), p. 575.
33. L. HELLER, P. SIGNELL, AND N. R. YODER, *Phys. Rev. Letters* **13**, 577 (1964).
34. R. P. HADDOCK, R. M. SALTER, JR., M. ZELLER, J. B. CZIRR, AND D. R. NYGREN, *Phys. Rev. Letters* **14**, 318 (1965).
35. H. P. NOYES, *Phys. Rev.* **130**, 2025 (1963).
36. G. BREIT, K. A. FRIEDMAN, AND R. E. SEAMON, *Suppl. Prog. Theoret. Phys.* (*Kyoto*) *Extra Number*, 449 (1965). See also H. P. NOYES, *Nucl. Phys.* **74**, 508 (1965).
37. T. L. HOUCK AND RICHARD WILSON, (private communication). The values quoted supersede their earlier results in Reference (*13*), p. 546.
38. T. HAMADA AND I. D. JOHNSTON, Reference (*11*) p. 388.
39. G. BREIT, K. A. FRIEDMAN, J. M. HOLT, AND R. E. SEAMON, *Phys. Rev.* **170**, 1424 (1968).
40. H. A. BETHE AND P. M. MORRISON, Reference (*31*), p. 93.
41. L. HELLER, Ref. (*13*) p. 584. The results quoted are for his quadratic fit.
42. J. W. KNOWLES, *Can. J. Physics* **40**, 257 (1962); W. V. PRESTWICH, T. J. KENNETT, L. B. HUGHS, AND J. FIEDLER, *ibid.* **43**, 2086 (1965); R. C. GREENWOOD AND W. W. BLACK, *Phys. Letters* **21**, 702 (1966). Note that Greenwood and Black correct the value of Knowles.

43. W. E. QUINN, J. M. BAKER, J. T. LATOURRETTE, AND N. F. RAMSEY, *Phys. Rev.* **112**, 1929 (1958).
44. G. F. NEWELL, *Phys. Rev.* **78**, 711 (1950).
45. J. P. AUFFRAY, *Phys. Rev. Letters* **6**, 120 (1961).
46. H. A. BETHE AND P. M. MORRISON, Reference (*31*), p. 106.
47. M. H. MACGREGOR, R. A. ARNDT AND R. M. WRIGHT, *Phys. Rev.* To appear.
48. R. E. SEAMON, K. A. FRIEDMAN, G. BREIT, R. D. HARACZ, J. M. HOLT, AND A. PRAKASH, Reference (*16*) p. 1583.
49. J. E. SIMMONS, Reference (*13*), p. 542.
50. F. COESTER AND E. YEN, *Nuovo Cimento* **30**, 674 (1963).
51. R. A. ARNDT AND M. H. MACGREGOR, These phase parameters are the ones from Reference (*24*) which we used for our $T = 1$ soft core potentials. The errors are unpublished early 1966 results. Results of more recent phase parameter searches (*16*), (*17*) are slightly different but not enough to affect our discussion in Section IV at all.
52. J. L. GAMMEL AND R. M. THALER, first paper in Reference (*9*).
53. J. L. GAMMEL AND R. M. THALER, Reference (*7*), p. 136. The example they give contains a misprint. As it stands it has a bound ^1S state.
54. T. HAMADA, *Prog. Theoret. Phys.* (*Kyoto*) **24**, 1033 (1960).
55. C. LEE, J. L. GAMMEL, AND R. M. THALER, "Nuclear Forces and the Few-Nucleon Problem" (T. C. Griffith and E. A. Power, Eds.), Vol. I, p. 43. Pergamon Press, London, 1960. See also J. L. GAMMEL AND R. M. THALER, Reference (*7*), p. 151.
56. D. A. GILTINAN AND R. M. THALER, *Phys. Rev.* **131**, 805 (1963).
57. N. R. YODER AND P. SIGNELL, *Prog. Theoret. Phys.* (*Kyoto*) **26**, 567 (1961).
58. H. P. NOYES, "Proceedings of the Second International Symposium on Polarization Phenomena of Nucleons," P. Huber and H. Schopper, Eds., p. 328. Birkhauser, Stuttgart, 1965.
59. R. TAMAGAKI AND W. WATARI, *Prog. Theoret. Phys.* (*Kyoto*), Suppl. **39**, 23 (1967).
60. T. HAMADA, *Prog. Theoret. Phys.* (*Kyoto*) **24**, 126 (1960).
61. T. HAMADA, *Prog. Theoret. Phys.* (*Kyoto*) **24**, 222 (1960).
62. T. HAMADA, *Prog. Theoret. Phys.* (*Kyoto*) **25**, 247 (1961).
63. R. A. ARNDT AND M. H. MACGREGOR (unpublished). These phase shifts are the ones of Reference (*28*) which we used for our $T = 0$ soft core potentials, and the errors are early 1966 results.
64. D. W. L. SPRUNG, private communication.

ANNALS OF PHYSICS: **50**, 449–471 (1968)

A Soluble Model of a Coupled Meson–Nucleon System

CARL B. DOVER*

Institut für theoretische Physik der Universität Heidelberg; W. Germany

An exactly soluble model, in which fermions in a many-body system interact through the exchange of a massive boson, is investigated. The model deals with the linear coupling of a neutral scalar meson field to fermion density fluctuations. These density fluctuations, or particle-hole excitations, are treated within the framework of the random phase approximation (RPA), while the meson degrees of freedom are treated exactly. Within the RPA, we obtain coupled oscillator equations of motion, which are subjected to a normal mode analysis. A dispersion relation for the normal mode energies is obtained, and the operators which create the properly "dressed" particle-hole and meson modes are constructed. The density-density correlation function and the meson Green's function are calculated exactly. The structure of the Green's functions is also explored from the point of view of their coupled equations of motion, which can be decoupled and solved in the RPA model. We also calculate the exact interaction energy, the scattering matrix for particle-hole pairs and the number of mesons produced by the interaction.

I. INTRODUCTION

The problem of nuclear structure is usually approached from the following viewpoint: Starting with a given free-space two-nucleon force (chosen phenomenologically to fit scattering phase shifts), one constructs an "effective interaction" (*1*), (*2*) appropriate to two nucleons embedded in a many-body system. This interaction is then utilized to calculate nuclear properties, such as energy spectra and transition rates.

However, the interaction between two nucleons is known to arise on the fundamental level from the exchange of quanta associated with various types of meson fields (*3*). In the above treatment, the meson degrees of freedom do not enter explicitly, their effect being simulated by the specified nucleon–nucleon potential (usually chosen to be static). It is hence natural to try to formulate a theory of nuclear systems in which mesons play an explicit role. A step in this general program was taken in Reference (*4*), in which the retarded nature of the two-nucleon interaction which results from meson exchange is explored. The

* Parts of this paper are based on a thesis submitted by C. B. Dover in partial fulfillment of the requirements for a Ph.D. degree in Physics, M.I.T., September, 1967. At M.I.T., the author was supported by a National Science Foundation predoctoral fellowship (1963–1967).

not obey a completeness relation. The whole theory of BHMM describes the missing part of the completeness relation. At best Ψ_p^+ is an eigenfunction of a complex Hamiltonian, which again does not obey (9). The analogue of Rodberg's equation (11) in the formalism of I is equation (4). There is no completeness relation for the $\mathbf{k}_p$ integration.

RECEIVED: May 1, 1968

REFERENCES

1. L. S. RODBERG, *Ann. Phys.* **48**, 254 (1968).
2. S. T. BUTLER, R. G. L. HEWITT, B. H. J. MCKELLAR, AND R. M. MAY, *Ann. Phys.* **43**, 282 (1967).
3. I. E. MCCARTHY, in preparation.
4. H. FESHBACH, *Ann. Phys.* **5**, 357 (1958).
5. A. J. KROMMINGA, K. L. LIM, AND I. E. MCCARTHY, *Phys. Rev.* **157**, 770 (1967).
6. S. T. BUTLER, *Ann. Phys.* **48**, 258 (1968).

ANNALS OF PHYSICS: **50**, 411–448 (1968)

Local Phenomenological Nucleon-Nucleon Potentials*†

RODERICK V. REID, JR.

Laboratory of Nuclear Science and Physics Department, Massachusetts Institute of Technology Cambridge, Massachusetts 02139
and
Cornell University, Physics Department, Ithaca, New York 14850

Hard (infinitely hard) and soft (Yukawa) core potentials have been fit to Yale and Livermore phase parameters and low-energy data. The potentials are local and static except that a different one is used for each state of distinct isotopic spin, total spin, and total angular momentum. It is found that neither the short-range behavior of the potentials nor the central-to-tensor ratio in the $^3S_1$–$^3D_1$ state is well determined by the data. Present data do exclude potentials containing only local central, tensor, and spin–orbit terms. Addition of a quadratic spin–orbit potential such as that used by the Yale group or by Hamada and Johnston helps greatly but is probably not enough to completely reproduce the data. Nevertheless, present day theories which use potentials are not likely to be sensitive to failures due to use of this form.

I. INTRODUCTION

The first experimental information bearing directly on the nucleon-nucleon (*NN*) interaction came from low-energy scattering done in the 1930's. The data had disappointingly little to say about the nature of the nuclear force. Almost any potential well with two adjustable parameters could be made to fit all low energy proton–proton (*pp*) data and a similar situation held in the neutron–proton (*np*) case.

In 1939 Rabi and co-workers (*1*) showed that the deuteron has an electric quadrupole moment. This single experimental result guaranteed that nuclei would be much more complicated structures than atoms for it implies that part of the *NN* interaction has a tensor character. Unfortunately, experimental data which give information concerning detailed characteristics of such forces are very hard to obtain. Even the quadrupole moment of the deuteron is not accurately known.

* This work was supported in part by a Cornell University fellowship, the U.S. Office of Naval Research, and the Atomic Energy Commission under contract AT(30-1)-2098.

† Part of this work was done in partial fulfillment of the requirements for the degree of Doctor of Philosophy at Cornell University.

In the late 1940's effective range theory explained the cause of the low energy "two-parameters-only" troubles. Due to the short range of the force, scattering below 5 MeV takes place with the nucleons almost entirely in an S-state and due to the strength of the force the energy dependence of the S-wave phase shift is adequately described by only two parameters (*2*).

Whereas at low energies the scattering process is frustratingly simple, at higher energies it is exasperatingly complicated. For example, the *pp* scattering matrix contains the known Coulomb amplitude plus five unknown, linearly independent, complex functions of the energy and scattering angle. Many varied and difficult experiments are required to determined the S-matrix (*3*). In 1953 Bethe (*4*) estimated that in the preceding quarter century more man hours of work had been devoted to the *NN* problem than to any other scientific question in the history of mankind.

The experimental effort increased further and in 1956 attempts to understand the data were made in two ways. Stapp, Ypsilantis and Metropolis (*5*) did a phase shift analysis at 310 MeV, the energy at which there was the most data. They found five satisfactory sets of phases. Thus there was still insufficient information to uniquely determine the S-matrix. Gammel, Christian and Thaler (*6*) tried to fit data at all energies with a static local potential of the form

$$V = V_C(r) + V_T(r)\, S_{12} \tag{1}$$

for each of the four possible combinations of isotopic spin and total spin. They failed. In Eq. (1), r is the distance between the nucleons, $V_C(r)$ is the central potential, $V_T(r)$ is the tensor potential and

$$S_{12} = 3(\sigma_1 \cdot \hat{r})(\sigma_2 \cdot \hat{r}) - \sigma_1 \cdot \sigma_2 \tag{2}$$

is the usual tensor operator. Such a sum of central and tensor terms is the most general form for a local potential which conserves total angular momentum, parity and charge, is time-reversal invariant, is charge independent and is completely independent of the relative momentum, $\mathbf{p}$ (*7*).

If the potential is allowed to depend at most linearly on $\mathbf{p}$ then a spin–orbit term can be added and

$$V = V_C(r) + V_T(r)\, S_{12} + V_{LS}(r)\, \mathbf{L} \cdot \mathbf{S} \tag{3}$$

This is the form originally proposed by Wigner (*8*). Since both S_{12} and $\mathbf{L} \cdot \mathbf{S}$ vanish in spin zero states the potential is not as complicated as it looks. There are four V_C's but only two V_T's and two V_{LS}'s. During the next year Gammel and Thaler (*9*) and Signell and Marshak (*10*) tried models of the Wigner type. The addition of spin–orbit forces resulted in significantly improved but not satisfactory fits to the data. In Section IV we discuss explicit areas of failure of this form.

In 1962 the two most widely used potentials appeared. Both abandoned the Wigner form. The Hamada and Johnston (*11*) (HJ) model used

$$V = V_C(r) + V_T(r)\, S_{12} + V_{LS}(r)\, \mathbf{L} \cdot \mathbf{S} + V_{LL}(r)\, L_{12}\,, \tag{4}$$

where

$$L_{12} = [\delta_{LJ} + (\sigma_1 \cdot \sigma_2)]\, \mathbf{L}^2 - (\mathbf{L} \cdot \mathbf{S})^2$$

and the Yale (*12*) potential used

$$V = V_C(r) + V_T(r)\, S_{12} + V_{LS}(r)\, \mathbf{L} \cdot \mathbf{S} + V_q(r)[(\mathbf{L} \cdot \mathbf{S})^2 + \mathbf{L} \cdot \mathbf{S} - \mathbf{L}^2]. \tag{5}$$

The HJ and Yale potentials represent vast improvements on all predecessors and give a semi-quantitative fit to the data.[1]

As the experimental situation improved, so did phase shift analyses. Two groups have done most of the work: one at Yale, led by Breit (*16*) and one at Livermore (*17*). Signell (*18*) and co-workers have also made a number of useful analyses.

In 1957 Moravcsik (*19*) made the suggestion that all phase shifts for partial waves with orbital angular momentum, L, greater than an appropriate maximum, $L_{\max}$, be taken directly from the theoretical one pion exchange amplitude. In recent work $L_{\max}$ is 5 and the one pion exchange contribution (OPEC) is used to get phases for $L \geqslant 6$. The one pion coupling constant, g^2, is treated as a parameter to be determined by the data. This procedure makes an enormous difference in the analysis because the data are not sufficiently abundant and accurate to fix all the high-L phases individually. Such use of the OPEC is best justified by the behavior of the free searched phases. As L increases towards $L_{\max}$ the phases approach corresponding OPEC phases of their own accord. Most important, by using the OPEC for high L phases, the phase shift solution for the lower L becomes unique, in contrast to the 5 solutions of Stapp et al. (*5*). It is also significant that g^2 tends to automatically take on a value of about 14 or 15 in agreement with that obtained from pion-nucleon scattering. From these properties Breit (*20*) and co-workers have shown that the corresponding one pion exchange potential (OPEP)

$$V^{\text{OPEP}} = (g^2/12)\, mc^2 (m/M)^2\, \tau_1 \cdot \tau_2 \left[\sigma_1 \cdot \sigma_2 + S_{12}\left(1 + \frac{3}{x} + \frac{3}{x^2}\right)\right] e^{-x}/x \tag{6}$$

[1] For other approaches to the *NN* problem see the minutes of the Conference on the *NN* Interaction (*13*) held at the University of Florida, Gainesville, Florida in March, 1967. A more recent and complete description of the boundary condition model of Lomon and Feshbach (*14*) is forthcoming (*15*).

constitutes most of the NN interaction at distances greater than about 3 Fermis. In Eq. (6) m is the pion mass, M is the nucleon mass, $\langle \tau_1 \cdot \tau_2 \rangle$ is 1 (−3) for isotopic spin 1 (0) and $x = \mu r$ with $\mu = mc/\hbar$.

The effort involved in phase shift analyses is massive. Nowadays in determining energy dependent phases in the range 0 — 350 MeV two thousand pieces of data are used after discarding a great many considered possibly unreliable. The results are gratifying. Only one set of phase shifts is emerging and the phases are fairly well determined. It is to these phase shifts that we have fit out potentials. We do not attempt to fit data above about 350 MeV. At higher energies pion production (with a 280 MeV threshold) and other relativistic effects become important and the two-nucleon Schrödinger equation inadequate.

The choice of our potential model is discussed in Section II. In Section III we compare our potentials with the HJ model, our phase shifts with the observed phases and our phase shifts with HJ phases. We also discuss the degree to which such potentials are unique. Section IV is devoted to restrictions on the functional form of a local potential imposed by the scattering data.

II. OUR POTENTIAL MODEL AND THE ASSOCIATED SCHRÖDINGER EQUATION

Desiring distinct potentials for each NN state in order that variations permitted by the data can be studied without simultaneously changing potentials in related states; we use in effect, a different central potential, $V(r)$, for each uncoupled state (states with total angular momentum, $J = L$ and the $^3P_0$ state). For each coupled state we adopt the form of Eq. (3). Such use of different local potentials for each NN state is by no means the most general form (*21*), (*22*), but if done for every state is sufficient in principle to reproduce all elastic scattering data. In this paper we focus our attention entirely on states with $J \leqslant 2$. These are the ones of overwhelming importance in nuclear physics. In the higher angular momentum states where we have given no potential one can either use experimental phase parameters[2] directly through a phase shift approximation (*23*) or use the OPEP. The phase shift approximation would probably be more accurate but is unnecessary[3] for many purposes.

At first glance it appears that our potential has more arbitrary parameters than the HJ or Yale versions and is therefore more complicated. In practice this is not so. For instance, in the singlet-even states, the HJ and Yale quadratic

[2] We recommend both the very nice recent Yale (*16*) and Livermore (*17*) results.

[3] Three possible exceptions are the $^1G_4$, $^3F_4$, and $^3D_3$ phase parameters. The experimental and OPEP values (in the approximations now used) for the $^3D_3$ differ even in sign. See Reference (*24*), Fig. 1.

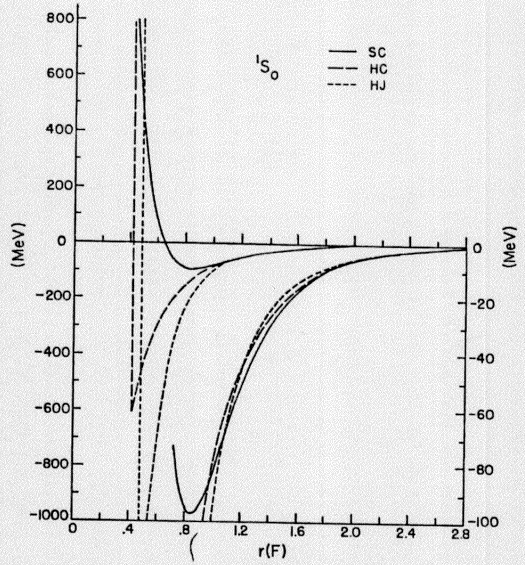

FIG. 1. Soft core (SC), hard core (HC), and Hamada–Johnston (HJ) $^1S_0$ potentials.

spin-orbit terms give different effective potentials for the ^1S and ^1D which is just what we assume. Explicitly, in singlet-even states

$$V(\text{HJ}, S = 0, T = 1) = V_C(r) - 2L(L+1)\, V_{LL}(r)$$
$$V(\text{Yale}, S = 0, T = 1) = V_C(r) - L(L+1)\, V_q(r) \qquad (7a)$$

V_{LL} and V_q are absent when $L = 0$, hence V_C can be chosen to fit the ^1S phase shift. If ^1D phases are calculated with V_C alone they turn out too attractive at high energies. Thus, a V_{LL} (or V_q) which gives a moderately short range repulsion will cause V to fit ^1D phases. The extra repulsion also tends to make ^1G phases turn out all right. Due to the large centrifugal barrier ^1G phases are not sensitive to details of the short range behavior. In fact, in the $^1G_4$ state almost any weak, medium range, attractive potential (added to the OPEP) will do. The other spin zero states, the singlet-odds, are all poorly determined by experiment. Yale puts $V_q = 0$ here.

For coupled states, the HJ V_{LL} merely changes their spin-orbit potential, V_{LS}, into $V_{LS} + V_{LL}$ and the Yale V_q does not appear at all; its factor in (5) is zero.

This reduces (5) to the form (3) which we use. Most of the experimental information on coupled states is concentrated on those with $J < 3$. But there is only one coupled state with $J = 1$, *viz.*, ${}^3S_1 - {}^3D_1$ and one coupled state with $J = 2$, *viz.*, ${}^3P_2 - {}^3F_2$. Since $T = 0$ and $T = 1$ potentials are different, we use no more potential components in the coupled states than HJ or Yale.

For the triplet states of $L = J$, notably ${}^3P_1$ and ${}^3D_2$, the quadratic spin-orbit terms do contribute. The effective potential (5) is

$$V(\text{Yale}, S = 1, L = J) = V_C + 2V_T - V_{LS} - L(L+1)\,V_q \qquad (7b)$$

and the HJ behaves similarly. The ${}^3P_1$ or ${}^3D_2$ potential can then be taken to be an arbitrary function of r, even if V_C, V_T and V_{LS} are completely given—it is only necessary to choose V_q appropriately. But V_q like all other components of the potential is assumed to depend on T and parity; therefore, e.g., the V_q for the ${}^3D_2$ state is independent of that for the ${}^1D$, and that for the ${}^3P_1$. This enables the Yale group and HJ to use, in the ${}^3D_2$ state the V_C, V_T, and V_{LS} previously derived from the ${}^3D_1 - {}^3S_1$ state and still have complete freedom to choose V for the ${}^3D_2$. This freedom is needed because, without V_q the ${}^3D_2$ potential (7b)

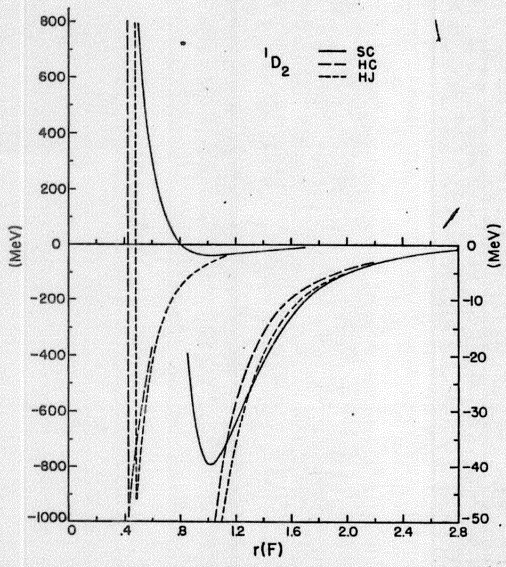

FIG. 2. Soft core (SC), hard core (HC), and Hamada–Johnston (HJ) ${}^1D_2$ potentials.

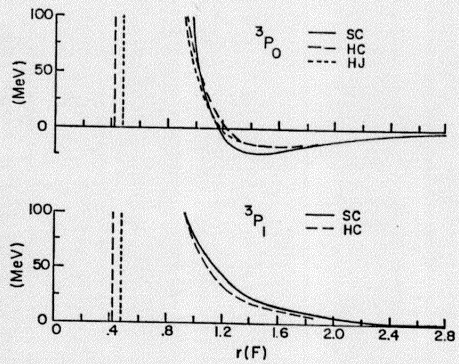

FIG. 3. Soft core (SC), hard core (HC) and Hamada–Johnston (HJ) ${}^3P_0$ and ${}^3P_1$ potentials. In the ${}^3P_1$ state the unplotted HJ curve falls slightly under the HC.

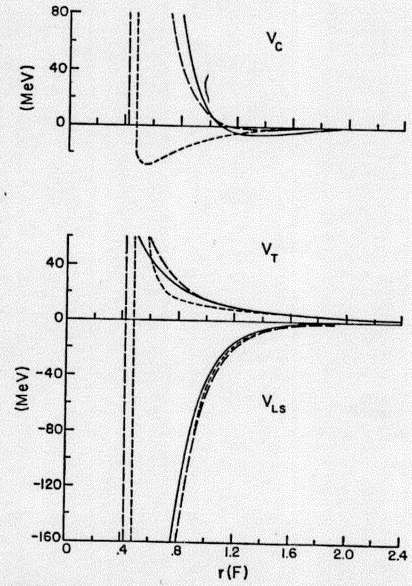

FIG. 4. Soft core (SC), hard core (HC) and Hamada–Johnston (HJ) ${}^3P_2$–${}^3F_2$ potentials. The HJ V_{LL} has been put into their V_{LS}.